Prototype-guided Cross-modal Completion and Alignment for Incomplete Text-based Person Re-identification

Tiantian Gong
Nanjing University of Aeronautics and Astronautics
Nanjing, China
tiantian_gong@nuaa.edu.cn

Guodong Du
Nanjing University of Aeronautics and Astronautics
Nanjing, China
andrew_du@foxmail.com

Junsheng Wang
Nanjing University of Science and Technology
Nanjing, China
jswang@njust.edu.cn

Yongkang Ding
Nanjing University of Aeronautics and Astronautics
Nanjing, China
ykding@nuaa.edu.cn

Liyan Zhang*
Nanjing University of Aeronautics and Astronautics
Nanjing, China
zhangliyan@nuaa.edu.cn

ABSTRACT

Traditional text-based person re-identification (ReID) techniques heavily rely on fully matched multi-modal data, which is an ideal scenario. However, due to inevitable data missing and corruption during the collection and processing of cross-modal data, the incomplete data issue is usually met in real-world applications. Therefore, we consider a more practical task termed the incomplete text-based ReID task, where person images and text descriptions are not completely matched and contain partially missing modality data. To this end, we propose a novel Prototype-guided Cross-modal Completion and Alignment (PCCA) framework to handle the aforementioned issues for incomplete text-based ReID. Specifically, we cannot directly retrieve person images based on a text query on missing modality data. Therefore, we propose the cross-modal nearest neighbor construction strategy for missing data by computing the cross-modal similarity between existing images and texts, which provides key guidance for the completion of missing modal features. Furthermore, to efficiently complete the missing modal features, we construct the relation graphs with the aforementioned cross-modal nearest neighbor sets of missing modal data and the corresponding prototypes, which can further enhance the generated missing modal features. Additionally, for tighter fine-grained alignment between images and texts, we raise a prototype-aware cross-modal alignment loss that can effectively reduce the modality heterogeneity gap for better fine-grained alignment in common space. Extensive experimental results on several benchmarks with different missing ratios amply demonstrate that our method can consistently outperform state-of-the-art text-image ReID approaches.

*Liyan Zhang is the corresponding author.

MM '23, October 29-November 3, 2023, Ottawa, ON, Canada

ACM ISBN 979-8-4007-0108-5/23/10…$15.00
https://doi.org/10.1145/3581783.3613802

CCS CONCEPTS

• **Information systems** → Multimedia and multimodal retrieval.

KEYWORDS

person re-identification, cross-modal alignment, incomplete modal data

ACM Reference Format:
Tiantian Gong, Guodong Du, Junsheng Wang, Yongkang Ding, and Liyan Zhang. 2023. Prototype-guided Cross-modal Completion and Alignment for Incomplete Text-based Person Re-identification. In *Proceedings of the 31st ACM International Conference on Multimedia (MM '23), October 29-November 3, 2023, Ottawa, ON, Canada.* ACM, New York, NY, USA, 9 pages. https://doi.org/10.1145/3581783.3613802

1 INTRODUCTION

Person re-identification (ReID) task aims at matching people images with the same identity across different cameras. ReID can be classified into three broad categories depending on the data type of the query object: image-based ReID [27, 33, 35], text-based person search [4, 7, 21] and video-based ReID [1, 10, 11, 17]. Text-based person (ReID) is a very challenging and significant task that aims to retrieve a person of interest through textual descriptions. Compared to its upstream task of image-based person re-identification [27, 28], it can handle the situation where the target pedestrian image cannot be obtained due to various reasons, but textual descriptions are available. Therefore, text-based ReID tasks have attracted increasing attention due to their practical significance, and are more challenging because of the dramatic modality gap.

Text-based ReID is a cross-modal fine-grained retrieval task, which aims to explore the fine-grained information between vision and language, as well as establish their alignment. Numerous effective text-image representation learning methods [26, 30, 31] have made great progress in recent years. These works follow a similar scheme: 1) This cross-modal alignment loss is adopted to align visual and textual representations into a common embedding space. 2) Text-based ReID models are trained on perfectly matched image-text pairs. They rely heavily on exactly matching image-text pairs, as shown in Figure 1 (a). The vast majority of text-based person re-identification assumes that the training instances at each

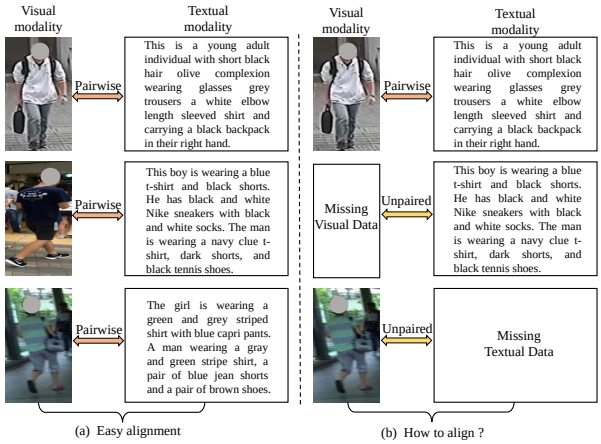

Figure 1: (a) Traditional text-image ReID approaches perform fine-grained alignment operations on fully matched image-text pair data, yet this is an ideal setting. Due to various inevitable errors, the incompletely matching multimodal data problem is often encountered in practical applications. (b) We therefore consider a more robust setting called incomplete text-image ReID.

modality and each category are sufficient and complete, i.e., pedestrian instances with the same identity contain both image modality and text modality. Indeed, this assumption cannot always be held in real-world applications. During multi-modal data acquisition and processing, data missing and corruption will inevitably occur. Consequently, previous methods that required complete modality data to construct ranking loss to explore text and image alignment could not work well in these scenarios. As shown in Figure 1 (b), the mismatch problem is common in text-based person datasets. In this work, we consider a more practical setting called an incomplete text-based person re-identification task, where only incomplete image-text pairs are available during the training phase.

Text-based ReID tasks are challenging due to the significant modality granularity gap and modality heterogeneity gap between vision and language, except for incomplete modality training data. The former challenge stems from the fact that visual features are usually fine-grained while textual features are coarse. Previous works investigated global alignment [24, 37, 39] to mitigate the modality granularity gap, which projects images and texts to a common embedding space to align them by designing cross-modal matching loss functions. Obviously, the global alignment methods ignore modality interactions when extracting features, which can not learn fine-grained local alignment. Thus, some works propose to align images and texts between parts of images and words of text and make great progress [5, 7, 23, 29, 38, 40]. However, different images and texts present different fine-grained features, and it is difficult to directly align them at the local level.

Obviously, incomplete text-based person re-identification has to address two problems: (1) How to handle incomplete modal training data? (2) How to align different fine-grained features across images and texts, and devise cross-modal alignment loss functions? To tackle the above issues and increase the robustness of incomplete text-based person retrieval for real-world applications. In this paper, we propose a novel prototype-guided cross-modal completion and alignment (PCCA) framework for incomplete text-based ReID. Especially, this PCCA framework consists of three modules: cross-modal nearest neighbors construction, prototype-based missing modal feature completion and prototype-aware cross-modal fine-grained alignment. Specifically, for missing visual (textual) modality data, we cannot directly calculate the similarity between them and other samples. Hence, we raise the cross-modal nearest neighbor construction method for the missing visual (textual) data by computing the cross-modal similarity between the existing textual (visual) samples and the existing visual (textual) samples to provide key information for missing modal feature completion. Moreover, for efficient missing modal feature completion, we leverage cross-modal neighbor sets of missing modal data and corresponding prototypes to model relational graphs, which can further enhance the reconstructed missing modal features. Besides, for compact fine-grained alignment between vision and language, we propose the multi-scale cross-modal unified prototype alignment that forces samples belonging to the same pedestrian identity to be closer in a common embedding space across different modalities through a multi-scale cross-modal unified prototype. Meanwhile, we exploit the cross-modal instance alignment loss to maximally maintain the mutual information between cross-modal image-text pairs in the common representation space. Extensive experimental results on several widely used text-based pedestrian datasets with different modality data missing rates fully demonstrate the superiority of our method compared to state-of-the-art text-image ReID methods.

Our key contributions are presented as follows:

- We propose a more robust text-to-image ReID task, termed the incomplete text-based ReID, which aims to efficiently identify target persons under incompletely matched image-text person training data. To the best of our knowledge, we are the first method that proposes an incomplete text-based re-identification task.
- For missing modal data, we present a cross-modal neighbor construction strategy and prototype-based relational graph modeling for reliable missing modal feature completion.
- To reduce the granularity gap between visual and textual modalities, we raise multi-scale unified prototype alignment, which can extract features with unified granularity from both modalities.
- Extensive experimental results on several incomplete benchmark datasets demonstrate that our proposed method can effectively handle text-based ReID in the face of numerous missing modal data, and outperforms several state-of-the-art text-based ReID methods.

2 RELATED WORK

2.1 Text-to-Image Person ReID

Different from the typical person ReID problems, text-based person ReID (TPReID) aims to identify the target person through free-form natural language. Compared with general cross-modal retrieval tasks, it is more challenging because of its fine-grained property. Learning discriminative alignment representations is the core of the TPReID task. According to whether there is an interaction scheme in

the process of learning cross-modal alignment, the existing methods can be roughly divided into two categories: cross-modal interaction-based and cross-modal interaction-free methods. The former [7, 21] mainly utilizes various attention-based models to establish region-word [2, 19, 20] or region-phrase [13, 21] correspondence relations, and predict the matching score for image-text pairs. For example, Niu et al. [21] employ the attention mechanism to carry out multi-granularity image-text alignment. Considering that aligning visual and textual clues across all scales is necessary, Gao et al. [7] propose a non-local alignment over full-cale representations that is able to adaptively align visual and textual features across all scales. Each coin has two sides. On the one hand, cross-modal interaction-based methods have the advantage of better aligning image-text embeddings and shrinking the modality gap through implicit cross-modal interaction. On the other hand, since the similarity scores between all local blocks are calculated during the interaction, the complexity of the cross-modal interaction-based methods is greatly increased. As a comparison, the latter [34, 37] mainly focuses on designing model structures and optimizing functions to learn aligned image and text embeddings in a joint latent space. For example, Zhang et al. [37] raise a cross-modal projection matching (CMPM) loss objection. The CMPM loss minimizes the KL divergence between the projection compatibility distributions and the normalized matching distributions defined with all the positive and negative samples in a mini-batch to maximize the compatibility of matched pairs for learning discriminative embeddings. Yan et al. [34] propose an implicit local alignment method to learn semantic alignment for image-text. More recent some Transformer-based methods [18, 26] have been proposed and achieved state-of-the-art performance.

2.2 Incomplete Cross-modal Retrieval

There is no work on the incomplete text-based person ReID problem. The most relevant to the incomplete text-based person ReID is the incomplete cross-modal retrieval (CMR) method [8, 12]. For example, literature [8] proposes a collective affinity learning method (CLAM), which constructs modality-specific bipartite graphs collectively and derives a probabilistic model to figure out complete data-to-anchor affinities for each modality, recovering the missing adjacency information. Literature [12] proposes a dual-aligned variational autoencoders (DAVAE) method to address the incomplete CMR problem, which enforces the latent features between image modality and text modality to be dual-aligned at the semantic level and the distribution level, and latent features are generated for the missing modalities. Although the abovementioned methods are all incomplete cross-modal retrievals, our incomplete text-based person ReID is fundamentally different from them, which lies in the following aspects: (1) CALM is an unsupervised hash-based method that cannot effectively utilize the label information to learn more discriminative features to reconstruct missing adjacency data. (2) DAVAE is a VAE-based [15] deep generative method that reconstructs incomplete samples via semantic consistency. However, on the one hand, it relies heavily on the semantic consistency of latent features when completing missing modal features and cannot make reasonable use of the neighbor semantic relationship between missing samples and existing samples. On the other hand, it fails to consider the modality gap in the reconstruction process. While our PCCA recovers missing modality features, not only the heterogeneity of modalities but also the semantic consistency of the cross-modal neighbors must be taken into account.

3 METHODOLOGY

Without losing generality, the traditional cross-modal complete image-text pairing data is represented as $\mathcal{X} = \{(x_k^v, x_k^t), y_k\}_{k=1}^N$, where x_k^v denotes the image modality instance, x_k^t denotes the text modality instance, and N is the number of all samples. In conventional cross-modal text-to-image person re-identification (ReID) tasks, the person images and their corresponding textual descriptions are typically given to be matched. However, this ideal assumption does not always hold in practical scenarios. Therefore, we work on exploring the modality alignment of incomplete text-based person re-identification data. For simplicity, we construct a matrix $A \in \mathbb{R}^{N\times 2}$ of N samples for both image-text modalities. If A_{i1}=0 or A_{j2}=0, $i \neq j$, then the ith visual modal instance or the jth textual modal instance is missing data, otherwise it is pairwise image-text data (A_{m1}=1 and A_{m2}=1). Further, we define that part completed data belong to the set $\mathcal{X}_p = \{(x_m^v, x_m^t)\}_{m=1}^{N'}$, and those data with missing visual modality only containing text data or missing textual modality only containing image data are collectively referred to as missing modality data and denoted as $\mathcal{X}_u^t = \{x_i^t\}_{i=1}^{N^t}$ and $\mathcal{X}_u^v = \{x_j^v\}_{j=1}^{N^v}$, $N' + N^v + N^t = N$.

3.1 Prototype-aware Cross-modal Completion

We first detail our feature extraction networks for visual and textual modalities. For each image data x_m^v and text data x_m^t, the visual representation $v_m^{'}$ as well as the textual representation $t_m^{'}$ can be obtained through visual encoder $f^v(x_m^v, \theta^v)$ with trainable parameters θ^v and textual encoder $f^t(x_m^t, \theta^t)$ with trainable parameters θ^t. In order to effectively fuse image and text representations, the text representation acts as query Q, the image representation acts as key K and value V, the image representation acts as Q, and the text representation acts as key K and value V. Therefore, the fused visual and textual feature representations can be formulated as follows,

$$v_m = Transformer(Q, K, V), \tag{1}$$

$$t_m = Transformer(Q, K, V), \tag{2}$$

where v_m and t_m represent the fused visual and text contextualized features. Specifically, we exploit the Transformer block operation to reconstruct visual and textual features, which consists of the multi-head cross attention MCA (self-attention for incomplete modal data) and feed-forward network FN, and $Transformer(Q, K, V) = FN(MCA(Q, K, V))$.

Next, we introduce the proposed prototype-aware cross-modal completion method for the incomplete text-based ReID, which includes cross-modal nearest neighbors construction and cross-modal missing features completion. Specifically, for the missing visual modality data $\mathcal{X}_u^t = \{x_i^t\}_{i=1}^{N^t}$ only with text data and missing textual modality data $\mathcal{X}_u^v = \{x_j^v\}_{j=1}^{N^v}$ only with image data, we need to reconstruct the missing visual features $\{\tilde{v}_i\}_{i=1}^{N^t}$ and the missing text features $\{\tilde{t}_j\}_{j=1}^{N^v}$ to ensure the integrity of the image-text pedestrian data. In order to effectively complement the missing modal representations, we first need to construct a cross-modal

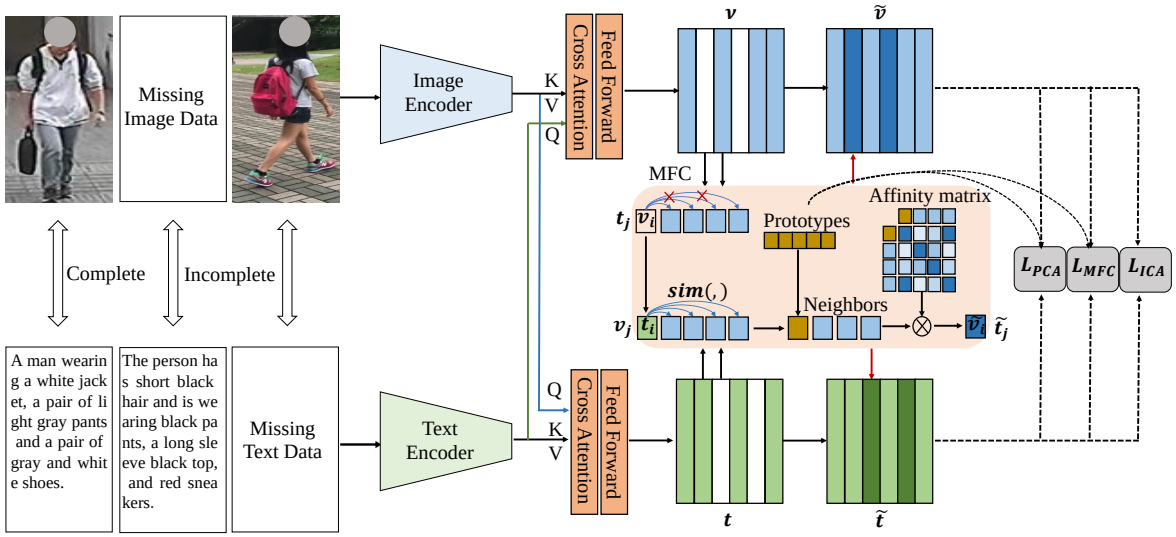

Figure 2: Illustration of a prototype-guided cross-modal completion and alignment framework (PCCA) for incomplete text-based person re-identification. It consists of visual and textual feature extraction networks, as well as prototype-based missing modal feature completion (MFC), prototype-based cross-modal alignment (PCA) and inter-instance cross-modal alignment (ICA). MFC is designed to model relational graphs for missing visual (textual) modal data by constructing cross-modal nearest neighbors and corresponding prototypes to enhance recovered features. Besides, we perform finer-grained alignment between images and texts by integrating multi-scale cross-modal unified prototype alignment as well as cross-modal instance alignment.

nearest neighbor set for the missing modal data by computing the cross-modal similarity between the existing textual (visual) samples and the existing visual (textual) samples, which provides the key clues for the completion of missing modal features. However, the construction of a cross-modal nearest neighbor set is extremely challenging because we cannot directly compute the similarity for missing modal data. To this end, we propose a cross-modal nearest neighbor construction and missing modality generation model.

Cross-modal Nearest Neighbors Construction. To reconstruct the missing modality representations, we need to establish a set of nearest neighbors for the missing image and text modality data. For simplicity, we use missing visual modality data as an example to detail our cross-modal nearest neighbors construction and cross-modal missing modality features completion. Specifically, for missing visual data $\tilde{x}_i^v$, we cannot directly calculate its distance from other existing visual data, but we can find existing text data x_i^t for $\tilde{x}_i^v$ in the corresponding text modality, and can obtain the textual representation t_i of x_i^t by the Eq (2), as illustrated in Figure 2. Further, we calculate the Euclidean distance between t_i and all existing image features v_i. Through the k-nearest neighbor function, we can get the k most similar visual embeddings to the textual representation t_i denoted by $N_k(t_i) = \{v_1, v_2, ..., v_k\}$. Symmetrically, we can also compute the nearest neighbors of missing text modality data defined as $N_k(v_j) = \{t_1, t_2, ..., t_k\}$, and obtain the set of near neighbors for all missing image and text modality data.

Missing Modal Features Completion. In order to effectively complete missing modality embeddings, we propose the missing modal feature completion (MFC) strategy, which needs to use the nearest neighbor sets of missing modal features and the cross-modal unified prototypes to construct the relationship graphs. Since samples from different modalities share the same semantic information [32, 36], the visual and textual modality unified prototypes are defined as $C = \{C_1, C_2, ..., C_Z\}, C_r = \{c_1, c_2, ..., c_M\}$, where Z multi-scale unified prototypes contain diverse semantic information, and M is the total number of pedestrian identities. The prototypes are randomly initialized, and the prototypes and common visual and textual representations are learned in the subsequent training process. For convenience, we use the prototype C_r as an example to illustrate the missing modal features completion (MFC) principle. For missing visual data $\tilde{x}_i^v$ and missing textual data $\tilde{x}_j^t$, we can obtain nearest neighbor sets $N_k(t_i) = \{v_1, v_2, ..., v_k\}$ and $N_k(v_j) = \{t_1, t_2, ..., t_k\}$ through the aforementioned cross-modal nearest neighbors construction method. The reconstructed image representation as well as the text representation are computed by,

$$\tilde{v}_i = A_v \cdot [c_l, N_k(t_i)], \quad \tilde{t}_j = A_t \cdot [c_n, N_k(v_j)], \tag{3}$$

where c_l represents the prototype with the same identity as t_i, c_n represents the prototype with the same identity as v_j, A_v is an affinity matrix of $[c_l, N_k(t_i)] = [c_l, v_1, v_2, ..., v_k]$, and A_t is an affinity matrix of $[c_n, N_k(v_j)] = [c_n, t_1, t_2, ..., t_k]$. Each element of the affinity matrix A_v (A_t) represents the degree of similarity between two samples, calculated as follows,

$$A_v = L^{-1} \cdot S^k, \tag{4}$$

where L^{-1} denotes the Laplacian matrix of S^k that is formulated as,

$$S_{ij} = \exp(sim(v_i, v_j)/\tau), \tag{5}$$

where we use the cosine similarity $sim(,)$ to calculate the similarity between two instances, and τ denotes the temperature hyperparameter set to 0.2. Further, we employ k-nearest neighbors to select

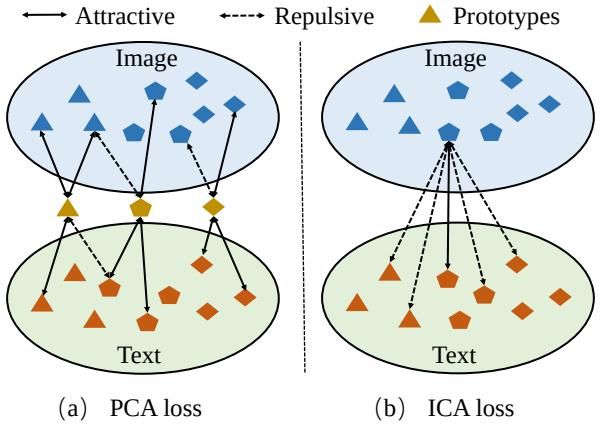

Figure 3: (a) Prototype-aware cross-modal alignment (PCA) loss is designed to classify image and text instances with the same pedestrian identity to its cross-modal unified prototype, which can better align global visual and textual embedding representations. (b) To maximally retain the mutual information between cross-modal image-text pairs in the common representation space, we utilize inter-instance cross-modal alignment (ICA) loss that aims to pull similar identity cross-modal instances closer while pushing away cross-modal samples from different identities.

the top k values at each row of the similarity matrix S defined as S^k. This method is essentially equivalent to constructing a graph relationship, and information can be transferred across different instances based on the graph, thereby enhancing features. To reduce the discrepancies between the generated missing-modal representations, the completed features can be better generated by pulling in the recovered features and their corresponding prototypes, and our proposed missing modal feature completion (MFC) is computed by,

$$L_{MFC}(\tilde{v}_i, c_l) = \|\tilde{v}_i - c_l\|_2^2, \tag{6}$$

$$L_{MFC}(\tilde{t}_j, c_n) = \|\tilde{t}_j - c_n\|_2^2. \tag{7}$$

3.2 Prototype-aware Cross-modal Alignment

To ensure samples belonging to the same pedestrian identity across different modalities are closer in common space, we raise a prototype-aware cross-modal alignment loss shown in Figure 3 (a) that can better align global visual and textual embeddings via cross-modal unified prototypes as a bridge. Specifically, for the given image representation v_i and text representation t_i, we classify v_i into its prototype c_l with the same identity and t_i into its prototype c_l with the same identity. The visual softmax probability $p(v_i, c_l)$ that v_i belongs to prototype c_l and the textual softmax probability $p(t_i, c_l)$ that t_i belongs to prototype c_l is defined as,

$$p(v_i, c_l) = \frac{\exp(v_i^\top c_l/\tau_1)}{\sum_{k=1}^{M}\exp(v_i^\top c_k/\tau_1)}, \tag{8}$$

$$p(t_i, c_l) = \frac{\exp(t_i^\top c_l/\tau_1)}{\sum_{k=1}^{M}\exp(t_i^\top c_k/\tau_1)}, \tag{9}$$

where c_l is the unified prototype, M is the total number of prototypes, and τ_1 is the class-level temperature factor set to 0.2. The prototype-aware cross-modal alignment (PCA) for visual and textual modalities can be implemented by optimizing two cross-entropy losses as follows,

$$L_i^v = -\sum_{l=1}^{M} 1\{y_i = l\}\log(p(v_i, c_l)), \tag{10}$$

$$L_i^t = -\sum_{l=1}^{M} 1\{y_i = l\}\log(p(t_i, c_l)), \tag{11}$$

where y_i is the true matching label. For all visual and textual representations, the overall PCA objective is optimized via,

$$L_{PCA} = \frac{1}{N}\sum_{i=1}^{N} L_i^v + \frac{1}{N}\sum_{i=1}^{N} L_i^t. \tag{12}$$

Our proposed PCA can efficiently classify instances with the same identity from different modalities closer to its prototype while pushing instances from different modalities with different identities away from the prototype.

3.3 Inter-instance Cross-modal Alignment

To enforce true image-text pairs closer while keeping all negative pairs farther apart, we employ the InfoNCE [22] loss as our inter-instance cross-modal alignment (ICA) loss from both image-to-text and text-to-image that can maximize the preservation of mutual information between cross-modal image-text pairs in the common representation space. Specifically, for a given embedded visual representation v_i as well as a textual representation t_i in a mini-batch containing B image-text pairs, the contrastive loss from image to text $L(v_i, t_i)$ and contrastive loss from text to image $L(t_i, v_i)$ respectively are computed as follows,

$$L(v_i, t_i) = 1_{y_{v_i}=y_{t_i}} \log\frac{\exp(sim(v_i, t_i)/\tau_2)}{\sum_{k=1}^{B}\exp(sim(v_i, t_k)/\tau_2)}, \tag{13}$$

$$L(t_i, v_i) = 1_{y_{t_i}=y_{v_i}} \log\frac{\exp(sim(t_i, v_i)/\tau_2)}{\sum_{k=1}^{B}\exp(sim(t_i, v_k)/\tau_2)}, \tag{14}$$

where τ_2 is the instance-level temperature factor set to 0.2, and B represents the batch size. $sim(,)$ denotes the cosine similarity shown as follows,

$$sim(v_i, t_i) = \frac{(v_i)^\top (t_i)}{\|(v_i)\|\|(t_i)\|}, \quad sim(t_i, v_i) = \frac{(t_i)^\top (v_i)}{\|(t_i)\|\|(v_i)\|}. \tag{15}$$

Therefore, the bidirectional instance-level cross-modal (ICA) loss for all visual and textual representations is defined as,

$$L_{ICA} = -\frac{1}{N}\sum_{i=1}^{N} L(v_i, t_i) - \frac{1}{N}\sum_{i=1}^{N} L(t_i, v_i). \tag{16}$$

3.4 Overall Objective

By combining the missing modal feature completion L_{MFC}, prototype aware cross-modal alignment L_{PCA} and instance-level cross-modal alignment L_{ICA}, our model (PCCA) can effectively recover missing modality representations and better learn aligned global

Table 1: Performance comparisons under three different settings on the CUHK-PEDES benchmark dataset.

Methods	Easy Setting (50%, 25%, 25%)			Medium Setting (30%, 35%, 35%)			Hard Setting (10%, 45%, 45%)		
	Rank-1	Rank-5	Rank-10	Rank-1	Rank-5	Rank-10	Rank-1	Rank-5	Rank-10
CMPM/C [37]	40.79	63.01	74.58	39.82	62.54	74.84	26.96	52.48	63.88
MIA [21]	46.23	68.56	77.64	43.64	66.37	74.11	29.78	54.94	65.71
SCAN [16]	49.84	71.96	79.38	46.87	69.43	77.64	31.83	53.77	64.93
ViTAA [29]	49.32	70.67	79.51	47.24	69.56	78.79	31.48	54.96	65.02
SSAN [5]	53.41	74.34	82.31	49.05	71.76	79.73	34.04	57.74	68.35
AXM-Net [6]	57.28	77.18	84.11	53.23	74.24	81.97	36.64	59.98	69.74
LGUR [26]	58.77	78.36	85.41	53.95	74.79	81.77	35.61	59.36	69.18
PCCA	**62.59**	**81.29**	**87.54**	**57.60**	**77.52**	**84.29**	**42.14**	**64.54**	**74.35**

Table 2: Performance comparisons under three different settings on the ICFG-PEDES benchmark dataset.

Methods	Easy Setting (50%, 25%, 25%)			Medium Setting (30%, 35%, 35%)			Hard Setting (10%, 45%, 45%)		
	Rank-1	Rank-5	Rank-10	Rank-1	Rank-5	Rank-10	Rank-1	Rank-5	Rank-10
CMPM/C [37]	34.69	55.86	65.71	29.73	51.17	60.84	15.62	30.26	41.59
MIA [21]	39.13	60.34	69.16	36.17	58.52	67.83	19.54	35.44	45.95
SCAN [16]	42.53	65.41	71.82	41.37	63.95	71.89	22.24	40.27	51.86
ViTAA [29]	43.79	65.86	73.42	42.78	64.55	72.41	22.61	40.62	51.37
SSAN[5]	46.27	67.06	75.52	44.86	66.72	74.58	24.83	42.64	53.19
AXM-Net[6]	50.31	70.62	77.93	48.26	67.14	76.69	28.26	49.53	59.49
LGUR[26]	52.73	70.55	78.41	48.32	68.73	76.91	29.73	51.26	60.19
PCCA	**54.68**	**72.91**	**80.88**	**51.46**	**71.05**	**77.93**	**35.46**	**56.84**	**66.93**

Table 3: Performance comparisons under three different settings on the RSTPReid benchmark dataset.

Methods	Easy Setting (50%, 25%, 25%)			Medium Setting (30%, 35%, 35%)			Hard Setting (10%, 45%, 45%)		
	Rank-1	Rank-5	Rank-10	Rank-1	Rank-5	Rank-10	Rank-1	Rank-5	Rank-10
CMPM/C [37]	32.81	56.90	67.51	29.50	54.11	65.16	17.04	38.31	48.71
MIA [21]	37.64	60.51	71.49	35.10	58.23	70.91	21.42	43.10	55.17
SCAN [16]	40.31	63.29	74.68	37.96	61.48	73.82	25.63	46.95	58.04
ViTAA [29]	40.73	63.34	75.81	37.29	61.46	74.21	24.85	45.97	57.96
SSAN [5]	42.38	63.52	76.89	39.61	63.97	75.12	26.83	47.57	58.46
AXM-Net [6]	42.62	64.54	77,40	39.91	64.02	76.47	25.43	46.67	57.58
LGUR[26]	44.03	65.66	78.15	41.69	65.02	77.53	27.91	48.73	59.97
PCCA	**46.89**	**68.80**	**78.94**	**43.71**	**66.94**	**78.39**	**33.71**	**54.50**	**63.19**

visual and textual embeddings in a joint latent space. Therefore, we train our model by minimizing the following loss,

$$L = L_{MFC} + L_{PCA} + L_{ICA}. \tag{17}$$

4 EXPERIMENTS

In this section, we first describe three widely used text-based person re-identification (ReID) datasets, new and challenging data partitions, and experimental evaluation settings for incomplete text-based ReID tasks. Then, we compare our method with state-of-the-art text-based ReID methods and conduct ablation experiments.

CUHK-PEDES [20] consists of 40,206 visual images as well as 80,412 text descriptions for 13,003 pedestrian identities. Each image contains at least two corresponding text descriptions. We follow the same data division as the literature [20]. The training data includes 34,054 image samples, 68,108 text descriptions, and 11,003 pedestrian identities. The test data contains 3,074 image instances and 6,156 text descriptions, with 1,000 person identities.

ICFG-PEDES [4] comprises 54,522 image samples with 4,102 different person identities. Each pedestrian image contains only one corresponding text description. The training data has 34674 image-text pair instances, including 3102 person identities. The test data consists of 19,848 image-text pair instances for 1,000 different identities.

RSTPReid [40] has 20505 images as well as 41010 textual descriptions for 4101 different person identities. Each identity contains 5 image samples taken by different cameras, where each image contains two corresponding text descriptions. We follow the same data division as the literature [40]. The dataset is divided into 3701, 200 and 200 pedestrian identities for training, testing, and validation, respectively.

New and Challenging Data Partitions. To implement incomplete text-based ReID experiments, we raise a new data splitting principle to divide the training data of the CUHK-PEDES, ICFG-PEDES, and RSTPReid datasets while keeping the test set the same as the previous methods. Specifically, we model the easy setting, medium setting, and hard setting with varying degrees of difficulty. For the easy setting, we allocate 50% as the complete text-image pedestrian data, 25% as missing visual modality data, and 25% as

Table 4: Performance comparisons by directly removing incomplete modal data on CUHK-PEDES benchmark dataset under the Easy setting.

Methods	Rank-1	Rank-5	Rank-10
SSAN [5]	53.41	74.34	82.31
AXM-Net [6]	57.28	77.18	84.11
LUGR [26]	58.77	78.36	85.41
PCCA (our)	**60.03**	**79.53**	**86.34**

Table 5: Performance comparisons by directly removing incomplete modal data on ICFG-PEDES benchmark dataset under the Easy setting.

Methods	Rank-1	Rank-5	Rank-10
SSAN [5]	46.27	67.06	75.52
AXM-Net [6]	50.31	70.62	77.93
LUGR [26]	52.73	70.55	78.41
PCCA (our)	**53.46**	**71.43**	**79.04**

missing textual modality data from the training set, denoted as (50%, 25%, 25%). Similarly, we define the medium setting as (30%, 35%, 35%) and the hard setting as (10%, 45%, 45%) to gradually increase the training difficulty.

Evaluation Protocols. We employ the Rank-k (k = 1, 5, 10) widely used in text-based ReID to evaluate the performance of the proposed method. Rank-k refers to the probability of identifying at least one pedestrian image within the top k candidates when given a textual query.

Implementation Details. In our experiments, we adopt ResNet-50 [9] as the visual backbone pre-trained on the ImageNet dataset [3] and the sequence of word embeddings extracted from BERT is then fed to Bi-LSTM [25]. During training, the image data is augmented with random horizontal flipping and all images are resized to 384 × 128. The temperature parameters τ_1, τ_2 and τ are set to 0.2. The model is optimized via the Adam optimizer [14] with a 0.0001 learning ratio. The batch size is 64, and the total number of epochs is 60. We execute all our experiments on a single 3090 24GB GPU.

4.1 Comparison with State-of-the-Art Methods

To fully demonstrate the effectiveness of our method (PCCA) for incomplete text-based person re-identification (ReID), we compare our method with several mainstream and state-of-the-art text-based person ReID methods. However, these methods are all performed on fully matched image-text pair datasets, which is inconsistent with our experimental setting of incomplete text-based ReID methods. Therefore, for a fair comparison, we reset these method settings to be consistent with ours. Specifically, these state-of-the-art text-based person ReID approaches include CMPM/C[37], MIA[21], SCAN[16], ViTAA[29], SSAN[5], AXM-Net[6] and LGUR[26].

Comparisons on Incomplete CUHK-PEDES. We first evaluate our proposed PCCA method on the most popular and widely-used benchmark dataset CUHK-PEDES. As shown in Table 1, our PCCA outperforms state-of-the-art text-based ReID methods in three different settings. Specifically, our PCCA achieves 62.59% , 57.60% and 42.14% Rank-1 accuracy, and surpasses the second highest LGUR method by 3.82%, 3.65% and 6.53% Rank-1 accuracy under three different settings, respectively. It can be observed that these text-based person ReID methods suffer significant performance degradation when encountering missing modal data. However, the performance drops more significantly when the missing data rate increases from the easy setting to the hard setting. Due to the large number of CUHK-PEDES dataset, there are still many complete image-text pair data available for training when 50% of the data is missing. Therefore, the experimental performances on the easy setting is not as outstanding as on the hard setting. Especially, the hard setting is the most challenging as only 10% of the data is complete and 90% of the data is incomplete including 45% missing visual modality data and 45% missing text modality data. In the hard setting, our method significantly outperforms the global matching LGUR method by 6.53%,5.18% and 5.17% on Rank-1, Rank-5 and Rank-10, respectively, which fully demonstrates that our proposed method can effectively explore incomplete missing data and improve the model robustness in practical application of text-based person re-identification.

Table 6: Ablation Study: Performance comparisons with different training sets on CUHK-PEDES dataset under the Medium setting.

Training Set Setting	Rank-1	Rank-5	Rank-10
only complete-modal data	54.24	74.89	82.35
dataset w/o image-modal data	55.91	75.97	83.33
dataset w/o text-modal data	55.87	75.98	83.31
the full dataset	**57.60**	**77.52**	**84.29**

Table 7: Ablation Study: Performance comparisons with different training sets on ICFG-PEDES dataset under the Medium setting.

Training Set Setting	Rank-1	Rank-5	Rank-10
only complete-modal data	49.12	69.73	77.23
dataset w/o image-modal data	50.16	69.59	77.55
dataset w/o text-modal data	50.08	69.53	77.46
the full dataset	**51.46**	**71.05**	**77.93**

Comparisons on Incomplete ICFG-PEDES. Next, we evaluate our proposed PCCA method on a new dataset ICFG-PEDES. As shown in Table 2, our PCCA consistently achieves the best performance on three different settings. Specifically, our PCCA achieves 54.68%, 51.46% and 35.46% Rank-1 accuracy, and surpasses the second highest LGUR method by 1.95%, 3.14% and 5.73% Rank-1 accuracy under three different settings, respectively. Especially in a difficult setting, the improvement brought by our method is significant, which means that it is particularly important to explore effective incomplete text-based REID methods. It can be observed that traditional text-based re-ReID methods do not perform well in the face of missing data.

In addition, we also evaluate the performance of our method without missing modal data on the CUHK-PEDES and ICFG-PEDES datasets under the easy setting. As shown in Table 4 and Table 5, comparing the performances of completing missing modal data in Table 1 and Table 2, directly removing incomplete modal data leads to a dramatic accuracy decline on Rank-1, Rank-5 and Rank-10,

Table 8: Ablation Study: Performance comparisons for four variants of PCCA on ICFG-PEDES dataset under the Hard setting.

Methods	Rank-1	Rank-5	Rank-10
PCCA w/o MFC	30.96	52.16	60.71
PCCA w/o PCA	29.74	51.61	60.64
PCCA w/o ICA	30.58	52.71	61.43
Full PCCA	**35.46**	**56.84**	**66.93**

respectively. This proves that it is extremely important to utilize incomplete modal data rather than discarding them directly. Although these data are incomplete, they still contain valuable information.

4.2 Ablation Studies

Analysis of Missing Modal Features Completion (MFC) As shown in Table 6 and Table 7, to verify the effectiveness of our missing modal feature completion, our method is trained under the medium setting on four different training sets, including setting 1) only complete modal data, 2) missing visual modality data, 3) missing textual modality data and 4) complete all missing modal data. It can be observed from these experimental results that the accuracy of Rank-1, Rank-5 and Rank-10 using only the complete modal data is the worst. As we reconstruct missing visual modality data or missing text modality data, experimental performance is gradually improved. The experimental performance reaches a maximum until all missing modal data are completed. Specifically, our PCCA with complete all missing modal data exceeds PCCA with only complete modal data by 3.36% and 2.34% Rank-1 accuracy under the medium setting on CUHK-PEDES and ICFG-PEDES datasets, respectively. This again verifies that our missing modal data completion method can effectively reduce the impact of performance degradation caused by numerous incomplete data.

Ablations on Available Components. To verify the effectiveness of each component in our PCCA method, we conduct experiments on ICFG-PEDES dataset under the hard setting with four different variants of PCCA, including 1) PCCA without missing modal features completion (MFC), 2) PCCA without prototype-aware cross-modal alignment (PCA), 3) PCCA without inter-instance cross-modal alignment (ICA) and 4) PCCA with all available components. As shown in Table 8, when our PCCA does not perform missing modal feature completion, the performance of our method decreases dramatically. This is because on the hard setting, very little data is available, severely affecting the Rank-1, Rank-5 and Rank-10 accuracy on ICFG-PEDES dataset. Specifically, our full PCCA surpasses PCCA without MFC by 4.5% Rank-1 accuracy under the hard setting on ICFG-PEDES dataset, respectively. This verifies that our proposed missing modal features completion (MFC) method can effectively recover the missing modal features and fully mine the valuable information of the missing modal data.

Further, when our PCCA does not execute prototype-based cross-modal alignment (PCA), its experimental results are far inferior to our full PCCA. Specifically, our full PCCA improves PCCA without PCA by 7.93% and 5.72% Rank-1 accuracy under the hard setting on the CUHK-PEDES and ICFG-PEDES datasets, respectively, which

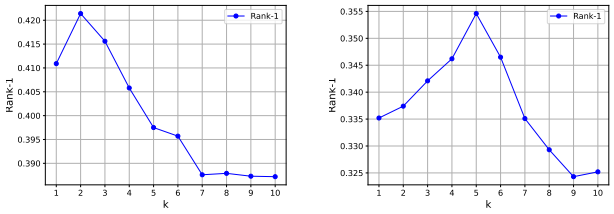

(a) CUHK-PEDES (b) ICFG-PEDES

Figure 4: Parameter analysis with the different nearest neighbor values k under the Hard setting on CUHK-PEDES and ICFG-PEDES datasets.

proves that our prototype-guided cross-modal alignment can effectively reduce fine-grained discrepancies across modalities through multi-scale cross-modal unified prototypes that act as a common bridge between visual and textual modalities.

In addition, when our PCCA does not implement inter-instance cross-modal alignment (ICA), our experimental results are far inferior to full PCCA. This indicates that our inter-instance cross-modal alignment can effectively preserve the alignment relationship between image-text pairs. It can be observed that our full PCCA achieves the best performance on the hard setting, thus demonstrating that our full PCCA can effectively handle the incomplete text-based person ReID problem when encountering numerous missing modal data to achieve tighter fine-grained alignment across modalities.

4.3 Parameter Analysis

In this section, we conduct hyperparameter analysis experiments under the hard setting on CUHK-PEDES and ICFG-PEDES datasets. As shown in Figure 4, we set the k value in the cross-modal nearest neighbor construction from 1 to 10. It can be observed that as the value of k increases, our Rank-1 accuracy first increases and then decreases, and reaches the maximum value when $k = 2$ on CUHK-PEDES as well as $k = 5$ on ICFG-PEDES. This shows that if the value of k is too large, it will increase the probability of false neighbors belonging to different pedestrian identities, resulting in a decrease in Rank-1 accuracy.

5 CONCLUSIONS

In this paper, we propose a novel prototype-guided cross-modal completion and alignment (PCCA) framework for the incomplete text-based person re-identification (ReID) task. Specifically, we raise the missing modal feature completion for missing data by exploiting the cross-modal nearest neighbor construction. In addition, we achieve a tighter fine-grained alignment between images and texts by integrating multi-scale prototype cross-modal alignment as well as cross-modal instance alignment. Extensive experimental results on several benchmarks fully demonstrate that our method can effectively handle the text-based person ReID problem in the face of numerous missing modal data.

ACKNOWLEDGMENTS

This work was supported in part by the National Natural Science Foundation of China under Grant 62172212.

REFERENCES

[1] Shutao Bai, Bingpeng Ma, Hong Chang, Rui Huang, and Xilin Chen. 2022. Salient-to-broad transition for video person re-identification. In *Proceedings of the IEEE/CVF Conference on Computer Vision and Pattern Recognition*. 7339–7348.

[2] Tianlang Chen, Chenliang Xu, and Jiebo Luo. 2018. Improving text-based person search by spatial matching and adaptive threshold. In *2018 IEEE Winter Conference on Applications of Computer Vision (WACV)*. IEEE, 1879–1887.

[3] Jia Deng, Wei Dong, Richard Socher, Li-Jia Li, Kai Li, and Li Fei-Fei. 2009. Imagenet: A large-scale hierarchical image database. In *2009 IEEE conference on computer vision and pattern recognition*. Ieee, 248–255.

[4] Changxing Ding, Kan Wang, Pengfei Wang, and Dacheng Tao. 2020. Multi-task learning with coarse priors for robust part-aware person re-identification. *IEEE Transactions on Pattern Analysis and Machine Intelligence* 44, 3 (2020), 1474–1488.

[5] Zefeng Ding, Changxing Ding, Zhiyin Shao, and Dacheng Tao. 2021. Semantically self-aligned network for text-to-image part-aware person re-identification. *arXiv preprint arXiv:2107.12666* (2021).

[6] Ammarah Farooq, Muhammad Awais, Josef Kittler, and Syed Safwan Khalid. 2022. AXM-Net: Implicit Cross-Modal Feature Alignment for Person Re-identification. In *Proceedings of the AAAI Conference on Artificial Intelligence*, Vol. 36. 4477–4485.

[7] Chenyang Gao, Guanyu Cai, Xinyang Jiang, Feng Zheng, Jun Zhang, Yifei Gong, Pai Peng, Xiaowei Guo, and Xing Sun. 2021. Contextual non-local alignment over full-scale representation for text-based person search. *arXiv preprint arXiv:2101.03036* (2021).

[8] Jun Guo and Wenwu Zhu. 2019. Collective affinity learning for partial cross-modal hashing. *IEEE Transactions on Image Processing* 29 (2019), 1344–1355.

[9] Kaiming He, Xiangyu Zhang, Shaoqing Ren, and Jian Sun. 2016. Deep residual learning for image recognition. In *Proceedings of the IEEE conference on computer vision and pattern recognition*. 770–778.

[10] Ruibing Hou, Hong Chang, Bingpeng Ma, Rui Huang, and Shiguang Shan. 2021. Bicnet-tks: Learning efficient spatial-temporal representation for video person re-identification. In *Proceedings of the IEEE/CVF conference on computer vision and pattern recognition*. 2014–2023.

[11] Ruibing Hou, Bingpeng Ma, Hong Chang, Xinqian Gu, Shiguang Shan, and Xilin Chen. 2019. Vrstc: Occlusion-free video person re-identification. In *Proceedings of the IEEE/CVF conference on computer vision and pattern recognition*. 7183–7192.

[12] Mengmeng Jing, Jingjing Li, Lei Zhu, Ke Lu, Yang Yang, and Zi Huang. 2020. Incomplete cross-modal retrieval with dual-aligned variational autoencoders. In *Proceedings of the 28th ACM International Conference on Multimedia*. 3283–3291.

[13] Ya Jing, Chenyang Si, Junbo Wang, Wei Wang, Liang Wang, and Tieniu Tan. 2020. Pose-guided multi-granularity attention network for text-based person search. In *Proceedings of the AAAI Conference on Artificial Intelligence*, Vol. 34. 11189–11196.

[14] Diederik P Kingma and Jimmy Ba. 2014. Adam: A method for stochastic optimization. *arXiv preprint arXiv:1412.6980* (2014).

[15] Diederik P Kingma and Max Welling. 2013. Auto-encoding variational bayes. *arXiv preprint arXiv:1312.6114* (2013).

[16] Kuang-Huei Lee, Xi Chen, Gang Hua, Houdong Hu, and Xiaodong He. 2018. Stacked cross attention for image-text matching. In *Proceedings of the European conference on computer vision (ECCV)*. 201–216.

[17] Jianing Li, Jingdong Wang, Qi Tian, Wen Gao, and Shiliang Zhang. 2019. Global-local temporal representations for video person re-identification. In *Proceedings of the IEEE/CVF international conference on computer vision*. 3958–3967.

[18] Shiping Li, Min Cao, and Min Zhang. 2022. Learning semantic-aligned feature representation for text-based person search. In *ICASSP 2022-2022 IEEE International Conference on Acoustics, Speech and Signal Processing (ICASSP)*. IEEE, 2724–2728.

[19] Shuang Li, Tong Xiao, Hongsheng Li, Wei Yang, and Xiaogang Wang. 2017. Identity-aware textual-visual matching with latent co-attention. In *Proceedings of the IEEE International Conference on Computer Vision*. 1890–1899.

[20] Shuang Li, Tong Xiao, Hongsheng Li, Bolei Zhou, Dayu Yue, and Xiaogang Wang. 2017. Person search with natural language description. In *Proceedings of the IEEE conference on computer vision and pattern recognition*. 1970–1979.

[21] Kai Niu, Yan Huang, Wanli Ouyang, and Liang Wang. 2020. Improving description-based person re-identification by multi-granularity image-text alignments. *IEEE Transactions on Image Processing* 29 (2020), 5542–5556.

[22] Aaron van den Oord, Yazhe Li, and Oriol Vinyals. 2018. Representation learning with contrastive predictive coding. *arXiv preprint arXiv:1807.03748* (2018).

[23] Tingting Qiao, Jing Zhang, Duanqing Xu, and Dacheng Tao. 2019. Mirrorgan: Learning text-to-image generation by redescription. In *Proceedings of the IEEE/CVF Conference on Computer Vision and Pattern Recognition*. 1505–1514.

[24] Nikolaos Sarafianos, Xiang Xu, and Ioannis A Kakadiaris. 2019. Adversarial representation learning for text-to-image matching. In *Proceedings of the IEEE/CVF international conference on computer vision*. 5814–5824.

[25] Mike Schuster and Kuldip K Paliwal. 1997. Bidirectional recurrent neural networks. *IEEE transactions on Signal Processing* 45, 11 (1997), 2673–2681.

[26] Zhiyin Shao, Xinyu Zhang, Meng Fang, Zhifeng Lin, Jian Wang, and Changxing Ding. 2022. Learning Granularity-Unified Representations for Text-to-Image Person Re-identification. In *Proceedings of the 30th ACM International Conference on Multimedia*. 5566–5574.

[27] Yifan Sun, Liang Zheng, Yi Yang, Qi Tian, and Shengjin Wang. 2018. Beyond part models: Person retrieval with refined part pooling (and a strong convolutional baseline). In *Proceedings of the European conference on computer vision (ECCV)*. 480–496.

[28] Kan Wang, Pengfei Wang, Changxing Ding, and Dacheng Tao. 2021. Batch coherence-driven network for part-aware person re-identification. *IEEE Transactions on Image Processing* 30 (2021), 3405–3418.

[29] Zhe Wang, Zhiyuan Fang, Jun Wang, and Yezhou Yang. 2020. Vitaa: Visual-textual attributes alignment in person search by natural language. In *Computer Vision–ECCV 2020: 16th European Conference, Glasgow, UK, August 23–28, 2020, Proceedings, Part XII 16*. Springer, 402–420.

[30] Zijie Wang, Aichun Zhu, Jingyi Xue, Xili Wan, Chao Liu, Tian Wang, and Yifeng Li. 2022. CAIBC: Capturing All-round Information Beyond Color for Text-based Person Retrieval. In *Proceedings of the 30th ACM International Conference on Multimedia*. 5314–5322.

[31] Zijie Wang, Aichun Zhu, Jingyi Xue, Xili Wan, Chao Liu, Tian Wang, and Yifeng Li. 2022. Look Before You Leap: Improving Text-based Person Retrieval by Learning A Consistent Cross-modal Common Manifold. In *Proceedings of the 30th ACM International Conference on Multimedia*. 1984–1992.

[32] Jianlong Wu, Zhouchen Lin, and Hongbin Zha. 2017. Joint latent subspace learning and regression for cross-modal retrieval. In *Proceedings of the 40th International ACM SIGIR Conference on Research and Development in Information Retrieval*. 917–920.

[33] Shiyu Xuan and Shiliang Zhang. 2021. Intra-inter camera similarity for unsupervised person re-identification. In *Proceedings of the IEEE/CVF conference on computer vision and pattern recognition*. 11926–11935.

[34] Shuanglin Yan, Hao Tang, Liyan Zhang, and Jinhui Tang. 2022. Image-specific information suppression and implicit local alignment for text-based person search. *arXiv preprint arXiv:2208.14365* (2022).

[35] Hong-Xing Yu, Wei-Shi Zheng, Ancong Wu, Xiaowei Guo, Shaogang Gong, and Jian-Huang Lai. 2019. Unsupervised person re-identification by soft multilabel learning. In *Proceedings of the IEEE/CVF conference on computer vision and pattern recognition*. 2148–2157.

[36] Zhixiong Zeng, Shuai Wang, Nan Xu, and Wenji Mao. 2021. Pan: Prototype-based adaptive network for robust cross-modal retrieval. In *Proceedings of the 44th International ACM SIGIR Conference on Research and Development in Information Retrieval*. 1125–1134.

[37] Ying Zhang and Huchuan Lu. 2018. Deep cross-modal projection learning for image-text matching. In *Proceedings of the European conference on computer vision (ECCV)*. 686–701.

[38] Kecheng Zheng, Wu Liu, Jiawei Liu, Zheng-Jun Zha, and Tao Mei. 2020. Hierarchical gumbel attention network for text-based person search. In *Proceedings of the 28th ACM International Conference on Multimedia*. 3441–3449.

[39] Zhedong Zheng, Liang Zheng, Michael Garrett, Yi Yang, Mingliang Xu, and Yi-Dong Shen. 2020. Dual-path convolutional image-text embeddings with instance loss. *ACM Transactions on Multimedia Computing, Communications, and Applications (TOMM)* 16, 2 (2020), 1–23.

[40] Aichun Zhu, Zijie Wang, Yifeng Li, Xili Wan, Jing Jin, Tian Wang, Fangqiang Hu, and Gang Hua. 2021. Dssl: Deep surroundings-person separation learning for text-based person retrieval. In *Proceedings of the 29th ACM International Conference on Multimedia*. 209–217.